Topological Yu-Shiba-Rusinov chain from spin-orbit coupling

P. M. R. Brydon, S. Das Sarma, Hoi-Yin Hui, and Jay D. Sau

Phys. Rev. B **91**, 064505 — Published 17 February 2015

DOI: 10.1103/PhysRevB.91.064505

Topological Yu-Shiba-Rusinov chain from spin-orbit coupling

P. M. R. Brydon,* S. Das Sarma, Hoi-Yin Hui, and Jay D. Sau
Condensed Matter Theory Center and Joint Quantum Institute,
University of Maryland, College Park, Maryland 20742-4111, USA
(Dated: January 22, 2015)

We investigate the possibility of realizing a topological state in the impurity band formed by a chain of classical spins embedded in a two-dimensional singlet superconductor with Rashba spin-orbit coupling. In contrast to similar proposals which require a helical spin texture of the impurity spins for a nontrivial topology, here we show that spin-flip correlations due to the spin-orbit coupling in the superconductor produces a topological state for ferromagnetic alignment of the impurity spins. From the Bogoliubov-de Gennes equations we derive an effective tight-binding model for the subgap states which resembles a spinless superconductor with long-range hopping and pairing terms. We evaluate the topological invariant, and show that a topologically non-trivial state is generically present in this model.

PACS numbers: 74.20.-z,75.70.Tj,73.63.Nm,03.67.Lx

I. INTRODUCTION

The search for a condensed-matter realization of the Majorana fermion continues, motivated both by the underlying fundamental physics and potential technological applications. Such states are predicted to occur in vortices of unconventional superconductors.[1] They may also be realized as edge states of engineered spinless superconductors with nontrivial topology, e.g. a Kitaev chain,[2] in a superconducting heterostructure.[3] Such a phase was predicted to occur in a semiconducting nanowire in proximity contact with a superconductor and in an applied magnetic field.[4,5] Transport signatures consistent with this theoretical prediction were subsequently detected,[6,7] although the definitive existence of the Majorana mode in such devices is still debated.[8]

Much attention has recently been directed at an alternative proposal, where a topological band arises from the overlapping Yu-Shiba-Rusinov (YSR) states[9] in a chain of magnetic impurities with helical spin order on the surface of a superconductor.[10–21] The helical spin texture plays a critical role combining the effect of the spin-orbit coupling (SOC) and external field in the nanowire proposal. Topological states are similarly predicted in metallic systems with coexisting superconductivity and helical magnetic order.[23–25] A significant advantage of the YSR chain proposal is that it is possible to unambiguously image the Majorana end modes using scanning tunneling microscopy (STM), in contrast to relying on difficult-to-interpret transport measurements of nanowire systems. Although critical to ensuring a topological state, the helical order also represents the main experimental difficulty since it is impossible to control externally. The helical order is stable when the magnetic ions are placed on a quasi-one-dimensional substrate,[12,14,16] but for the physically-relevant case of a planar surface the chain is generically unstable towards a ferromagnetic or antiferromagnetic configuration.[26] A pair-breaking effect in the superconducting state might nevertheless restore the stability of the helical order,[20] but disorder effects may still turn out to be a strong detrimental factor.[26]

The prospect of unambiguously verifying the existence of Majorana end modes in a YSR chain motivates the search for a way to realize a topological state in this system without relying upon an intrinsic helical ordering of the impurity spins. For example, it has been proposed to use external magnetic fields and a supercurrent flow to tune a nontopological antiferromagnetic chain into a topological regime.[22] In view of the importance of SOC in the nanowire proposal, it is also interesting to include SOC in the description of the superconducting host of the impurity chain. Indeed, one typically expects the presence of a Rashba SOC at the surface of the superconductor due to the broken inversion symmetry. We note that SOC intrinsic to the superconductor has been considered in other proposals for realizing topological systems,[27] and the possible relevance of SOC in the context of a topologically nontrivial magnetic impurity chains has been mentioned in Ref. 26. This scenario has recently been invoked to explain STM measurements of zero-bias peaks at the ends of a ferromagnetic chain on a superconductor,[28] although the relevance of YSR physics to this situation is uncertain, as we discuss below. In spite of the extensive activity on the interplay between magnetic chains and superconductivity in generating emergent topological phases,[10–22] the specific problem of combining both spin-orbit coupling and magnetic YSR chain physics together in a model has been conspicuously lacking. We study this particular issue in our current work by generalizing and synthesizing the existing work in the literature, most specifically Refs. 10, 13, and 26.

We mention here that very recently there has been a spurt in the activity[29–32] on topological superconductivity and emergent Majorana fermions, following Ref. 28, in ferromagnetic chains fabricated on the surface of bulk superconductors. In particular, a report of impressive STM experiments[29] has just appeared claiming the generic observation of Majorana fermions at the ends of Fe chains on superconducting Pb. These experiments are the main reason for this enhanced activity, but the question of the topological nature of purely ferromagnetic chains proximity coupled to s-wave superconductors is of intrinsic theoretical interest independent of experimental developments. Rather surprisingly, the theory of such systems has not yet been dealt with in any detail, in contrast to the extensive theoretical analyses of spiral YSR chains and spin-polarized semiconducting nanowires. Although there is superficial similarity between the model used in the current work and the experimental systems,[28,29] it is far too early to tell whether there is any connection between the theory and predictions presented in the current work involving a weakly coupled YSR chain and the experimental system involving Fe chains where tunneling between the atoms may well be strong. The corresponding topological theory for strongly-coupled ferromagnetic chains on superconducting substrates has been considered in Refs. 29–32, and is a generalization of previous proposals to realize Majorana fermions in half-metals (i.e. fully spin-polarized ferromagnets) deposited on superconductors.[27] Further discussion of such strongly tunnel coupled ferromagnetic nanowire systems and the experimental results of Ref. 29 is beyond the scope of the current work.

In this paper we show that the SOC indeed induces a topological state in a YSR chain formed from ferromagnetically aligned impurity spins, and so demonstrate that the more delicate helical order is not essential to such proposals. To this end, we analytically construct a tight-binding model for the YSR states valid in the limit of "deep" impurities, when the impurity band lies close to the middle of the superconducting gap. Although the SOC does not affect the YSR states for an isolated impurity, it dramatically alters the results for the chain. Specifically, spin-flip correlations in the bulk superconductor, induced by the antisymmetric SOC, mix the two branches of the impurity band when the polarization of the impurity spins is transverse to the SOC along the chain. This can be interpreted as a triplet pairing amplitude in a Kitaev-like model, and is thus responsible for the topologically nontrivial state. A magnetic polarization parallel to the SOC, on the other hand, produces no such mixing but instead results in an asymmetric dispersion with trivial topology. We construct a phase diagram, demonstrating that a topological state is possible for infinitesimal SOC strength. Our analysis closely follows that of Ref. 13, where a similar tight-binding model for the impurity band was obtained for a chain with spiral magnetic texture embedded in a three-dimensional superconductor.

II. MODEL

A bulk two-dimensional singlet s-wave superconductor with Rashba SOC is described by the Hamiltonian $H = \sum_{\mathbf{k}} \Psi_{\mathbf{k}}^{\dagger} \check{H}_{\mathbf{k}} \Psi_{\mathbf{k}}$ where

$$\check{H}_{\mathbf{k}} = \hat{\tau}_z \otimes (\xi_{\mathbf{k}} \hat{\sigma}_0 + \mathbf{l}_{\mathbf{k}} \cdot \hat{\boldsymbol{\sigma}}) + \Delta \hat{\tau}_x \otimes \hat{\sigma}_0 \,. \tag{1}$$

Here $\hat{\tau}_\mu$ ($\hat{\sigma}_\mu$) are the Pauli matrices in Nambu (spin) space, and $\Psi_{\mathbf{k}} = (c_{\mathbf{k},\uparrow}, c_{\mathbf{k},\downarrow}, c^{\dagger}_{-\mathbf{k},\downarrow}, -c^{\dagger}_{-\mathbf{k},\uparrow})^T$ is the spinor of creation and annihilation operators. We have adopted the notation that $\hat{\ldots}$ and $\check{\ldots}$ indicate 2×2 and 4×4 matrices, respectively. The noninteracting dispersion is given by $\xi_{\mathbf{k}} = \hbar^2\mathbf{k}^2/2m - \mu$ where m is the effective mass and μ the chemical potential, the Rashba SOC is parametrized by $\mathbf{l}_{\mathbf{k}} = \lambda(k_y \mathbf{e}_x - k_x \mathbf{e}_y) = \lambda k(\sin\theta \mathbf{e}_x - \cos\theta \mathbf{e}_y)$ where λ is the SOC strength, and Δ is the superconducting gap.

The SOC lifts the spin degeneracy in the normal state, resulting in the dispersions $\xi_{\mathbf{k},\pm} = \xi_{\mathbf{k}} \pm |\mathbf{l}_{\mathbf{k}}|$, where the plus (minus) sign corresponds to the positive (negative) helicity band. As time-reversal symmetry remains intact, however, in the superconducting phase there is only pairing between states in the same helicity band. The bulk Green's function can then be written as $\check{G}_{\mathbf{k}}(\omega) = \frac{1}{2}\{\check{G}^{+}_{\mathbf{k}}(\omega) + \check{G}^{-}_{\mathbf{k}}(\omega)\}$, where

$$\check{G}^{\pm}_{\mathbf{k}}(\omega) = (\omega\hat{\tau}_0 + \xi_{\pm}\hat{\tau}_z + \Delta\hat{\tau}_x) \otimes (\hat{\sigma}_0 \pm \sin\theta\hat{\sigma}_x \mp \cos\theta\hat{\sigma}_y) \times \left(\omega^2 - \xi_{\pm}^2 - \Delta^2\right)^{-1} \,, \tag{2}$$

is the Green's function in each helicity sector. Note that the SOC produces normal spin-flip and triplet pairing terms in the Green's function.[33] For clarity we suppress the momentum index in the dispersion of the helical bands, i.e. $\xi_{\mathbf{k},\pm} \equiv \xi_{\pm}$.

III. SINGLE IMPURITY

We first consider a single (classical) magnetic impurity with spin $\mathbf{S}$ at the origin, interacting with the electron states with exchange strength $-J$. We include this in our model by adding $H_{\mathrm{imp}} = -J\mathbf{S} \cdot [\Psi^{\dagger}(\mathbf{0})\hat{\tau}_0 \otimes \hat{\boldsymbol{\sigma}}\Psi(\mathbf{0})]$ to the bulk Hamiltonian, where $\Psi(\mathbf{r}) = \int \frac{d^2k}{(2\pi)^2} \Psi_{\mathbf{k}} e^{i\mathbf{k}\cdot\mathbf{r}}$. We aim to solve the Bogoliubov-de Gennes equation $(H + H_{\mathrm{imp}})\psi(\mathbf{r}) = \omega\psi(\mathbf{r})$ for the impurity bound states, i.e. for energy $|\omega| < \Delta$. By straightforward manipulation,[13] the spinor of the bound state at the impurity $\psi(\mathbf{0})$ satisfies the equation

$$\left\{ \check{1} + \int \frac{d^2k}{(2\pi)^2} \check{G}_{\mathbf{k}}(\omega) J\mathbf{S} \cdot (\hat{\tau}_0 \otimes \hat{\boldsymbol{\sigma}}) \right\} \psi(\mathbf{0}) = 0 \,. \tag{3}$$

To evaluate this equation, we split the Green's function into positive and negative helicity components and then convert the integral over the momentum to an integral over the appropriate dispersion $\xi_{\pm}$ and the angle θ

$$\int \frac{d^2k}{(2\pi)^2} \check{G}^{\pm}_{\mathbf{k}}(\omega) \approx \frac{\mathcal{N}_{\pm}}{2\pi} \int_{-D}^{D} d\xi_{\pm} \int_0^{2\pi} d\theta \check{G}^{\pm}_{\mathbf{k}}(\omega) \,, \tag{4}$$

where $\mathcal{N}_{\nu} = (m/\pi\hbar^2)[1 \mp \widetilde{\lambda}/(1 + \widetilde{\lambda}^2)^{1/2}]$ is the density of states of the $\nu = \pm$ helicity band at the Fermi level, $\widetilde{\lambda} = \lambda m/\hbar k_F$ is the ratio of SOC splitting to the Fermi energy and gives a dimensionless measure of the SOC strength, k_F the Fermi wavevector in the absence of SOC, and $D \to \infty$ is a cutoff. The symmetric cutoff in Eq. (4) is used for simplicity; Although it implies particle-hole symmetry of the normal dispersion, relaxing this assumption does not qualitatively change our results. The resulting integrals are presented in the appendix. Due to the isotropic δ-function structure of the potential, the integrals involving the spin-flip and triplet pairing terms in the Green's function vanish, and Eq. (3) therefore has exactly the same form as a magnetic impurity in an s-wave superconductor without SOC,[9,13] specifically

$$\left\{\check{1} - \frac{\alpha}{\sqrt{\Delta^2-\omega^2}}\left[\omega\hat{\tau}_0 + \Delta\hat{\tau}_x\right]\otimes(\mathbf{e_S}\cdot\hat{\boldsymbol{\sigma}})\right\}\psi(\mathbf{0}) = 0\,, \quad (5)$$

where $\alpha = \frac{\pi}{2}(\mathcal{N}_+ + \mathcal{N}_-)JS$, $S = |\mathbf{S}|$, and $\mathbf{e_S} = \mathbf{S}/S$. The solutions of this equation occur at $\omega = \pm\epsilon_0$, where $\epsilon_0 = \Delta(1-\alpha^2)/(1+\alpha^2)$. The form of the corresponding spinors $\psi_\pm(\mathbf{0})$ is dictated by the orientation of the impurity spin. Parametrizing $\mathbf{S} = S(\cos\eta\sin\zeta, \sin\eta\sin\zeta, \cos\zeta)$, these spinors can then be written[13] up to unimportant normalization constant as

$$\psi_+(\mathbf{0}) = \begin{pmatrix}\chi_\uparrow\\ \chi_\uparrow\end{pmatrix}, \qquad \psi_-(\mathbf{0}) = \begin{pmatrix}\chi_\downarrow\\ -\chi_\downarrow\end{pmatrix}, \quad (6)$$

where

$$\chi_\uparrow = \left(\ \cos\zeta/2\,,\ \ e^{i\eta}\sin\zeta/2\ \right)^T\,, \quad (7)$$

$$\chi_\downarrow = \left(\ e^{-i\eta}\sin\zeta/2\,,\ \ -\cos\zeta/2\ \right)^T\,. \quad (8)$$

IV. FERROMAGNETIC CHAIN

The above analysis can be extended to a chain of ferromagnetically-aligned impurity spins, with the impurity Hamiltonian now written as

$$\mathcal{H}_{\text{imp}} = -J\sum_j \mathbf{S}\cdot\left[\Psi^\dagger(\mathbf{r}_j)\hat{\tau}_0\otimes\hat{\boldsymbol{\sigma}}\Psi(\mathbf{r}_j)\right]\,, \quad (9)$$

where $\mathbf{r}_j$ is the position of the jth impurity. We have suppressed the site index of the spins since they all point in the same direction. Without loss of generality, we assume that the chain runs along the x-axis, and so $\mathbf{r}_j = x_j\mathbf{e}_x$. After similar manipulations as in the single impurity problem, the BdG equations for the subgap YSR states on the chain can be written

$$\left\{\check{1} - \frac{\alpha}{\sqrt{\Delta^2-\omega^2}}\left[\omega\hat{\tau}_0 + \Delta\hat{\tau}_x\right]\otimes(\mathbf{e_S}\cdot\hat{\boldsymbol{\sigma}})\right\}\psi(x_i) = -\sum_{j\neq i}\check{J}(x_{ij})\mathbf{e_S}\cdot(\hat{\tau}_0\otimes\hat{\boldsymbol{\sigma}})\psi(x_j) \quad (10)$$

where $x_{ij} = x_i - x_j$ and the matrix $\check{J}(x_{ij})$ is defined

$$\begin{aligned}\check{J}(x_{ij}) &= JS\int\frac{d^2k}{(2\pi)^2}\check{G}_{\mathbf{k}}(\omega)e^{ik_x x_{ij}}\\ &= \frac{JS}{2}\left\{[I_1^-(x_{ij}) + I_1^+(x_{ij})]\hat{\tau}_z\otimes\hat{\sigma}_0 + \omega[I_3^-(x_{ij}) + I_3^+(x_{ij})]\hat{\tau}_0\otimes\hat{\sigma}_0 + \Delta[I_3^-(x_{ij}) + I_3^+(x_{ij})]\hat{\tau}_x\otimes\hat{\sigma}_0\right.\\ &\quad\left. + [I_2^-(x_{ij}) - I_2^+(x_{ij})]\hat{\tau}_z\otimes\hat{\sigma}_y + \omega[I_4^-(x_{ij}) - I_4^+(x_{ij})]\hat{\tau}_0\otimes\hat{\sigma}_y + \Delta[I_4^-(x_{ij}) - I_4^+(x_{ij})]\hat{\tau}_x\otimes\hat{\sigma}_y\right\}\,. \end{aligned} \quad (11)$$

We have expressed this in terms of the integrals

$$I_1^\nu(x) = \frac{\mathcal{N}_\nu}{2\pi}\int_{-D}^{D}d\xi\int_0^{2\pi}d\theta\frac{\xi e^{ik_\nu(\xi)x\cos\theta}}{\omega^2-\xi^2-\Delta^2}\,, \quad (12a)$$

$$I_2^\nu(x) = \frac{\mathcal{N}_\nu}{2\pi}\int_{-D}^{D}d\xi\int_0^{2\pi}d\theta\frac{\xi e^{i\theta}e^{ik_\nu(\xi)x\cos\theta}}{\omega^2-\xi^2-\Delta^2}\,, \quad (12b)$$

$$I_3^\nu(x) = \frac{\mathcal{N}_\nu}{2\pi}\int_{-D}^{D}d\xi\int_0^{2\pi}d\theta\frac{e^{ik_\nu(\xi)x\cos\theta}}{\omega^2-\xi^2-\Delta^2}\,, \quad (12c)$$

$$I_4^\nu(x) = \frac{\mathcal{N}_\nu}{2\pi}\int_{-D}^{D}d\xi\int_0^{2\pi}d\theta\frac{e^{i\theta}e^{ik_\nu(\xi)x\cos\theta}}{\omega^2-\xi^2-\Delta^2}\,, \quad (12d)$$

where $k_\nu(\xi) = k_{F,\nu} + \xi/\hbar v_{F,\nu}$, while $k_{F,\nu} = k_F[(1+\widetilde{\lambda}^2)^{1/2} - \nu\widetilde{\lambda}]$ and $v_{F,\nu} = (\hbar k_F/m)(1+\widetilde{\lambda}^2)^{1/2}$ are the Fermi vector and velocity for the ν helicity band, respectively. These integrals are explicitly evaluated in the appendix for $D\to\infty$, where we also provide asymptotic expansions valid for $k_{F,\nu}|x| \gg 1$. Note that $I_1^\nu(x)$ and $I_3^\nu(x)$ are even functions of x, whereas $I_2^\nu(x)$ and $I_4^\nu(x)$ are odd.

In contrast to the single-impurity system considered above, the presence of SOC makes a significant difference to the BdG equations for the multi-impurity problem: while the first line of Eq. (11) is identical to the result found in Ref. 13, the second line is only present for nonzero SOC. This line contains explicitly magnetic terms $\propto \hat{\sigma}_y$, reflecting the orientation of the SOC vector $\mathbf{l_k}||\mathbf{e}_y$ for $\mathbf{k}$ pointing along the magnetic chain.

V. TIGHT-BINDING MODEL

We do not attempt a general solution of Eq. (10), but instead consider the analytically-tractable limit of dilute "deep" impurities, as discussed in Ref. 13. Specifically, we assume that $\alpha \approx 1$, so that the energy ϵ_0 of the isolated YSR state lies close to the center of the gap, and that the spacing a between impurities is sufficiently large that the impurity band formed from the hybridized YSR states lies entirely within the superconducting gap. Linearizing the BdG equations Eq. (10) in the energy ω and the coupling between impurity sites, we obtain after straightforward manipulation

$$\Delta\left[\mathbf{e_S}\cdot(\hat{\tau}_0\otimes\hat{\boldsymbol{\sigma}})-\alpha\hat{\tau}_x\otimes\hat{\sigma}_0\right]\psi(x_i)+\Delta\sum_{j\neq i}\mathbf{e_S}\cdot(\hat{\tau}_0\otimes\hat{\boldsymbol{\sigma}})\lim_{\omega\to 0}\check{J}(x_{ij})\mathbf{e_S}\cdot(\hat{\tau}_0\otimes\hat{\boldsymbol{\sigma}})\psi(x_j)=\omega\psi(x_i) \tag{13}$$

This equation is now projected into the YSR states [Eq. (6)] at each site, to obtain a BdG-type equation for the impurity band

$$\widetilde{H}(i,j)\phi_j=\omega\phi_i \tag{14}$$

where $\phi_i=(u_{i,+},u_{i,-})^T$ is the vector of the wavefunctions for the + and − YSR states at site i and

$$\widetilde{H}(i,j)=\begin{pmatrix} A_{ij}+B_{ij} & C_{ij} \\ C^*_{ji} & -A_{ij}+B_{ij}\end{pmatrix} \tag{15}$$

where

$$A_{ij}=\epsilon_0\delta_{ij}+\frac{1}{2}JS\Delta^2\lim_{\omega\to 0}\left[I_3^+(x_{ij})+I_3^-(x_{ij})\right], \tag{16}$$

$$B_{ij}=\frac{1}{2}JS\Delta^2\sin\eta\sin\zeta\lim_{\omega\to 0}\left[I_4^-(x_{ij})-I_4^+(x_{ij})\right], \tag{17}$$

$$C_{ij}=-\frac{i}{2}JS\Delta\left(\cos^2\tfrac{\zeta}{2}+\sin^2\tfrac{\zeta}{2}e^{-2i\eta}\right)\times\lim_{\omega\to 0}\left[I_2^-(x_{ij})-I_2^+(x_{ij})\right]. \tag{18}$$

Note that the integrals in these expressions are to be regarded as vanishing for $i=j$.

The effective tight-binding Hamiltonian Eq. (15) is the central result of this paper. Due to the antisymmetry of the integrals $I_2^\nu(x)$ in the off-diagonal terms, it can be interpreted as describing superconducting spinless fermions, recalling the Kitaev model,[2] albeit with long-range hopping and pairing terms. The properties of this system depend crucially on the SOC in the bulk superconductor and the polarization of the impurity spins. Specifically, the pairing term C_{ij} is only present for nonvanishing SOC, and when the polarization of the ferromagnetic chain has a component perpendicular to the y-axis. Examining Eq. (11), we observe that the pairing term originates from the spin-flip correlations in the host superconductor induced by the SOC. A polarization component along the y-axis contributes an antisymmetric hopping B_{ij} in the presence of SOC. This echoes the asymmetric dispersion of a spin-orbit coupled electron gas in the direction of an applied magnetic field, and its appearance here is due to the triplet pairing correlations in the bulk Green's function Eq. (2).

A similar tight-binding model was derived in Ref. 13, but there the odd-parity pairing term arose from the spiral magnetic texture of the impurity chain. This mechanism for generating a pairing term is still valid in the presence of the SOC considered here. Examining the interplay of spiral spin texture and SOC is an interesting topic which we leave to later work.

VI. TOPOLOGICAL PROPERTIES

To conclude we examine the topology of the impurity band. For an infinite chain with uniform spacing a of the impurities, we define the Fourier transform of the Hamiltonian Eq. (15)

$$\widetilde{H}(k)=\begin{pmatrix} A(k)+B(k) & C(k) \\ C^*(k) & -A(k)+B(k)\end{pmatrix} \tag{19}$$

where $A(k)=\sum_j A_{0j}e^{ikja}$, etc. Using the asymptotic forms for the integrals, it is possible to obtain analytical expressions for these quantities in the limit $k_{F,\nu}a\gg 1$, which are presented in the appendix. The Hamiltonian Eq. (19) is in Altland-Zirnbauer symmetry class D, and for a fully-gapped system it is therefore characterized by the $\mathbb{Z}_2$ topological invariant[2]

$$Q=\mathrm{sgn}\{A(0)A(\pi/a)\}. \tag{20}$$

The system is topologically nontrivial for $Q=-1$; conversely, $Q=1$ indicates a trivial state.

To demonstrate that our model supports a topologically nontrivial state, in Fig. (1) we present a phase diagram as a function of the dimensionless SOC $\widetilde{\lambda}$ and the parameter k_Fa, which gives a measure of the Fermi surface volume or alternatively the spacing of the chain. We consider only a polarization in the x-z plane. In the topologically non-trivial regions, we plot the minimum gap magnitude, demonstrating the existence of a fully gapped state; the non-topological regions are left white. The most important aspect of this phase diagram is that a topological state is revealed to be possible even for infinitesimal SOC. Remarkably, the excitation spectrum can display a substantial gap even for very small SOC strength $\widetilde{\lambda}\ll 1$. We emphasize that our analysis is only valid for ϵ_0 sufficiently close to zero, and so other methods are required to comprehensively survey the phase diagram.

VII. SUMMARY

In this paper we have studied the appearance of a topological impurity band when a ferromagnetic chain of classical spins are embedded in a two-dimensional singlet s-wave superconductor with Rashba SOC. To this end, we have derived an effective tight-binding model for the overlapping YSR states of the impurities. When the spins are polarized perpendicular to the SOC along the chain, an

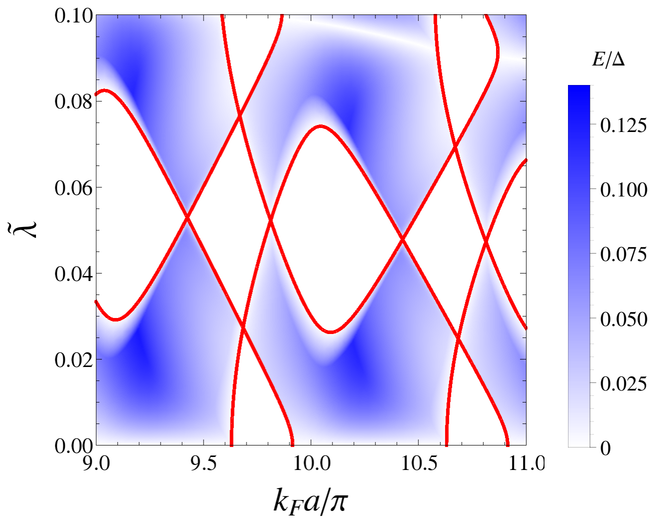

FIG. 1. (Color online). Topological phase diagram for the effective model as a function of $k_F a$ and $\widetilde{\lambda}$. The topological regions are shaded according to the magnitude of the gap, while the nontopological regions are left blank. Red lines indicate the boundary between topological and nontopological phases. We have chosen $\epsilon_0 = 0$ for the isolated impurity level and $\xi_0 = 5a$ for the superconducting coherence length at $\widetilde{\lambda} = 0$, which ensures that the impurity band remains within the superconducting gap. The impurity spins point in the x-z plane. The large values of $k_F a$ allow us to utilize the asymptotic expressions for the entries in Eq. (19).

odd-parity pairing term is induced in the effective Hamiltonian, thus realizing a Kitaev-like model with generically non-trivial topology. Our work and recent others[22] explore alternative routes to a topological YSR chain which do not rely upon helical spin texture.[10–21] This is a significant result, as the stability of the helical spin texture is debated.[20,26] In contrast, the SOC mechanism examined here is intrinsic to the superconductor surface. This implies that topological phases are possible for a much wider variety of impurity spin configurations than hitherto realized, which grants the YSR chain proposal additional robustness and lends strong theoretical support to experimental efforts to detect Majorana fermions in such a setting. As revealed by our calculated quantum phase diagram Fig. (1), however, the topological phase in the ferromagnetic YSR chain system is not generic. Some fine-tuning of the system is therefore required in order to observe topological Majorana fermions through the measurement, for example, of zero-bias-conductance peaks in tunneling spectroscopy experiments.

Although we have confined ourselves to the analytically-tractable limit of a dilute chain of deep impurities, we expect that our results are of more general validity since they rely only upon the low-energy form of the Green's function. We have also neglected complicating factors such as particle-hole asymmetry in the normal state dispersion, the suppression of the superconducting gap close to the impurity spins, and the three-dimensional nature of the superconducting host. These issues must certainly be accounted for when modelling a realistic system, but can only be addressed using large-scale computer simulations. Nevertheless, none of these effects should invalidate the mechanism giving rise to the topological state of our basic model which arises simply from the interplay between ferromagnetism, superconductivity, and SOC.

ACKNOWLEDGMENTS

The authors thank P. Kotetes and A. Yazdani for useful discussions. This work is supported by JQI-NSF-PFC and LPS-CMTC.

Appendix A: Important integrals

In this appendix we present analytic forms for the four integrals Eq. (12) encountered in our solution of the YSR chain. We perform by these integrals by extending the cutoff $D \to \infty$. We distinguish two cases for the argument: $x = 0$ for the isolated YSR impurity, and $x \neq 0$ for the YSR chain.

1. Isolated impurity: $x = 0$

In this case all the integrals except $I_3^\nu(0)$ are vanishing, which evaluates to

$$I_3^\nu(0) = \frac{\pi \mathcal{N}_\nu}{\sqrt{\Delta^2 - \omega^2}}\,. \tag{A1}$$

2. Impurity chain: $x \neq 0$

For $x \neq 0$, we first evaluate the integral over ξ using elementary contour integral methods, and then evaluate the angular integral. We hence find

$$I_1^\nu(x) = \pi \mathcal{N}_\nu \mathrm{Im}\left\{J_0((k_{F,\nu} + i\xi_\nu^{-1})|x|) + iH_0((k_{F,\nu} + i\xi_\nu^{-1})|x|)\right\}\,, \tag{A2}$$

$$I_2^\nu(x) = -i\pi \mathcal{N}_\nu\,\mathrm{sgn}(x)\mathrm{Re}\left\{iJ_1((k_{F,\nu} + i\xi_\nu^{-1})|x|) + H_{-1}((k_{F,\nu} + i\xi_\nu^{-1})|x|)\right\}\,, \tag{A3}$$

$$I_3^\nu(x) = -\frac{\pi \mathcal{N}_\nu}{\sqrt{\Delta^2 - \omega^2}}\mathrm{Re}\left\{J_0((k_{F,\nu} + i\xi_\nu^{-1})|x|) + iH_0((k_{F,\nu} + i\xi_\nu^{-1})|x|)\right\}\,, \tag{A4}$$

$$I_4^{\nu}(x) = -\,\mathrm{sgn}(x)\frac{i\pi\mathcal{N}_\nu}{\sqrt{\Delta^2-\omega^2}}\mathrm{Im}\left\{iJ_1((k_{F,\nu}+i\xi_\nu^{-1})|x|)+H_{-1}((k_{F,\nu}+i\xi_\nu^{-1})|x|)\right\}\,, \tag{A5}$$

where $J_n(z)$ and $H_n(z)$ are Bessel and Struve functions of order n, respectively, and $\xi_\nu = \hbar v_{F,\nu}/\sqrt{\Delta^2-\omega^2}$. Using asymptotic forms[34] valid for large values of the argument close to the positive real axis, we can approximate these as

$$I_1^{\nu}(x) \approx \pi\mathcal{N}_\nu\sqrt{\frac{2}{\pi k_{F,\nu}|x|}}\sin\left(k_{F,\nu}|x|-\tfrac{\pi}{4}\right)e^{-|x|/\xi_\nu}+\frac{2\mathcal{N}_\nu}{k_{F,\nu}|x|}\,, \tag{A6}$$

$$I_2^{\nu}(x) \approx i\pi\mathcal{N}_\nu\,\mathrm{sgn}(x)\sqrt{\frac{2}{\pi k_{F,\nu}|x|}}\sin\left(k_{F,\nu}|x|-\tfrac{3\pi}{4}\right)e^{-|x|/\xi_\nu}+\mathrm{sgn}(x)\frac{2i\mathcal{N}_\nu}{(k_{F,\nu}x)^2}\,, \tag{A7}$$

$$I_3^{\nu}(x) \approx -\frac{\pi\mathcal{N}_\nu}{\sqrt{\Delta^2-\omega^2}}\sqrt{\frac{2}{\pi k_{F,\nu}|x|}}\cos\left(k_{F,\nu}|x|-\tfrac{\pi}{4}\right)e^{-|x|/\xi_\nu}\,, \tag{A8}$$

$$I_4^{\nu}(x) \approx -\,\mathrm{sgn}(x)\frac{i\pi\mathcal{N}_\nu}{\sqrt{\Delta^2-\omega^2}}\sqrt{\frac{2}{\pi k_{F,\nu}|x|}}\cos\left(k_{F,\nu}|x|-\tfrac{3\pi}{4}\right)e^{-|x|/\xi_\nu}\,. \tag{A9}$$

The nonoscillating component is valid up to $\mathcal{O}((k_{F,\nu}|x|)^{-3})$.

3. Fourier transforms

The Fourier transform of the effective Hamiltonian Eq. (15) can be carried out analytically when we utilize the asymptotic expressions. Defining the Fourier transform as

$$A(k) = \sum_j A_{0j}e^{ikja}\,, \tag{A10}$$

we obtain

$$\begin{aligned}I_2^{\nu}(k) = {} & \mathcal{N}_\nu\sqrt{\frac{\pi}{2k_{F,\nu}a}}\left\{e^{-3\pi i/4}\mathrm{Li}_{\frac{1}{2}}\left(e^{i(k_{F,\nu}a+ka)-a/\xi_\nu}\right)-e^{3\pi i/4}\mathrm{Li}_{\frac{1}{2}}\left(e^{i(-k_{F,\nu}a+ka)-a/\xi_\nu}\right)\right.\\ & \left.-e^{-3\pi i/4}\mathrm{Li}_{\frac{1}{2}}\left(e^{i(k_{F,\nu}a-ka)-a/\xi_\nu}\right)-e^{3\pi i/4}\mathrm{Li}_{\frac{1}{2}}\left(e^{i(-k_{F,\nu}a-ka)-a/\xi_\nu}\right)\right\}\\ & +\frac{2i\mathcal{N}_\nu}{(k_{F,\nu}a)^2}\left\{\mathrm{Li}_2\left(e^{ika}\right)-\mathrm{Li}_2\left(e^{-ika}\right)\right\}\,, \end{aligned} \tag{A11}$$

$$\begin{aligned}I_3^{\nu}(k) = {} & -\frac{\mathcal{N}_\nu}{\sqrt{\Delta^2-\omega^2}}\sqrt{\frac{\pi}{2k_{F,\nu}a}}\left\{e^{-\pi i/4}\mathrm{Li}_{\frac{1}{2}}\left(e^{i(k_{F,\nu}a+ka)-a/\xi_\nu}\right)+e^{\pi i/4}\mathrm{Li}_{\frac{1}{2}}\left(e^{i(-k_{F,\nu}a+ka)-a/\xi_\nu}\right)\right.\\ & \left.+e^{-\pi i/4}\mathrm{Li}_{\frac{1}{2}}\left(e^{i(k_{F,\nu}a-ka)-a/\xi_\nu}\right)+e^{\pi i/4}\mathrm{Li}_{\frac{1}{2}}\left(e^{i(-k_{F,\nu}a-ka)-a/\xi_\nu}\right)\right\}\,, \end{aligned} \tag{A12}$$

$$\begin{aligned}I_4^{\nu}(k) = {} & -\frac{i\mathcal{N}_\nu}{\sqrt{\Delta^2-\omega^2}}\sqrt{\frac{\pi}{2k_{F,\nu}a}}\left\{e^{-3\pi i/4}\mathrm{Li}_{\frac{1}{2}}\left(e^{i(k_{F,\nu}a+ka)-a/\xi_\nu}\right)+e^{3\pi i/4}\mathrm{Li}_{\frac{1}{2}}\left(e^{i(-k_{F,\nu}a+ka)-a/\xi_\nu}\right)\right.\\ & \left.-e^{-3\pi i/4}\mathrm{Li}_{\frac{1}{2}}\left(e^{i(k_{F,\nu}a-ka)-a/\xi_\nu}\right)-e^{3\pi i/4}\mathrm{Li}_{\frac{1}{2}}\left(e^{i(-k_{F,\nu}a-ka)-a/\xi_\nu}\right)\right\}\,, \end{aligned} \tag{A13}$$

where $\mathrm{Li}_s(z)$ is the polylogarithm of order s.

* pbrydon@umd.edu

[1] N. Read and D. Green, Phys. Rev. B **61**, 10267 (2000); S. Das Sarma, C. Nayak, and S. Tewari, Phys. Rev. B **73**, 220502(R) (2006); C. Zhang, S. Tewari, R. M. Lutchyn, and S. Das Sarma, Phys. Rev. Lett. **101**, 160401 (2008); M. Sato and S. Fujimoto, Phys. Rev. B **79**, 094504 (2009); P. Hosur, P. Ghaemi, R. S. K. Mong, and A. Vishwanath, Phys. Rev. Lett. **107**, 097001 (2011).

[2] A. Y. Kitaev, Phys. Usp. **44**, 131 (2001).
[3] L. Fu and C. L. Kane, Phys. Rev. Lett. **100**, 096407 (2008); J. D. Sau, R. M. Lutchyn, S. Tewari, and S. Das Sarma, *ibid* **104**, 040502 (2010); J. D. Sau, S. Tewari, R. M. Lutchyn, T. Stanescu, and S. Das Sarma, Phys. Rev. B **82**, 214509 (2010).
[4] R. M. Lutchyn, J. D. Sau, and S. Das Sarma, Phys. Rev. Lett. **105**, 077001 (2010).
[5] Y. Oreg, G. Refael, and F. von Oppen, Phys. Rev. Lett. **105**, 177002 (2010).
[6] V. Mourik, K. Zuo, S. M. Frolov, S. R. Plissard, E. P. A. M. Bakkers, and L. P. Kouwenhoven, Science **336**, 1003 (2012).
[7] A. Das, Y. Ronen, Y. Most, Y. Oreg, M. Heiblum, and H. Shtrikman, Nature Phys. **8**, 887 (2012).
[8] D. Bagrets and A. Altland, Phys. Rev. Lett. **109**, 227005 (2012); D. I. Pikulin, J. P. Dahlhaus, M. Wimmer, H. Schomerus, and C. W. J. Beenakker, New. J. Phys. **14**, 125011 (2012).
[9] L. Yu, Acta Phys. Sin. **21**, 75 (1965); H. Shiba, Prog. Theor. Phys. **40**, 435 (1968); A. I. Rusinov, Zh. Eksp. Teor. Fiz. Pisma. Red. **9**, 146 (1968) [JETP Lett. **9**, 85 (1969)].
[10] T.-P. Choy, J. M. Edge, A. R. Akhmerov, and C. W. J. Beenakker, Phys. Rev. B **84**, 195442 (2011).
[11] S. Nadj-Perge, I. K. Drozdov, B. A. Bernevig, and A. Yazdani, Phys. Rev. B **88**, 020407(R) (2013).
[12] B. Braunecker and P. Simon, Phys. Rev. Lett. **111**, 147202 (2013).
[13] F. Pientka, L. I. Glazman, and F. von Oppen, Phys. Rev. B **88**, 155420 (2013).
[14] J. Klinovaja, P. Stano, A. Yazdani, and D. Loss, Phys. Rev. Lett. **111**, 186805 (2013).
[15] S. Nakosai, Y. Tanaka, and N. Nagaosa, Phys. Rev. B **88** 180503 (2013).
[16] M. M. Vazifeh and M. Franz, Phys. Rev. Lett. **111**, 206802 (2013).
[17] K. Pöyhönen, A. Westström, J. Röntynen, and T. Ojanen, Phys. Rev. B **89**, 115109 (2014).
[18] F. Pientka, L. I. Glazman, and F. von Oppen, Phys. Rev. B **89**, 180505(R) (2014).
[19] J. Röntynen and T. Ojanen, Phys. Rev. B **90**, 180503(R) (2014).
[20] I. Reis, D. J. J. Marchand, and M. Franz, Phys. Rev. B **90**, 085124 (2014).
[21] S. Nadj-Perge, I. Drozdov, S. Jeon, J. Seo, A. Bernevig, and A. Yazdani, Bull. Am. Phys. Soc. **58**, Z46.10 (2014).
[22] A. Heimes, P. Kotetes, and G. Schön, Phys. Rev. B **90**, 060507(R) (2014).
[23] M. Kjaergaard, K. Wölms, and K. Flensberg, Phys. Rev. B **85**, 020503(R) (2012).
[24] I. Martin and A. F. Morpurgo, Phys. Rev. B **85**, 144505 (2012).
[25] P. Kotetes, New J. Phys. **15**, 105027 (2013).
[26] Y. Kim, M. Cheng, B. Bauer, R. M. Lutchyn, and S. Das Sarma, Phys. Rev. B **90**, 060401(R) (2014).
[27] P. A. Lee, arXiv:0907.2681; M. Duckheim and P. W. Brouwer, Phys. Rev. B **83**, 054513 (2011); S.-B. Chung, H.-J. Zhang, X.-L. Qi, and S.-C. Zhang, *ibid* **84**, 060510(R) (2011).
[28] A. Yazdani, Nobel Symposium 156 on New Forms of Matter: Topological Insulators and Superconductors, Sweden, June 12-15 (2014) .
[29] S. Nadj-Perge, I. K. Drozdov, J. Li, H Chen, S. Jeon, J. Seo, A. H. MacDonald, B. A. Bernevig, and A. Yazdani, Science **346**, 602 (2014).
[30] H.-Y. Hui, P. M. R. Brydon, J. D. Sau, S. Tewari, and S. Das Sarma, arXiv:1407.7519.
[31] J. Li, H. Chen, I. K. Drozdov, A. Yazdani, B. A. Bernevig, and A.H. MacDonald, Phys. Rev. B **90**, 235433 (2014).
[32] E. Dumitrescu, B. Roberts, S. Tewari, J. D. Sau, and S. Das Sarma, arXiv:1410.5412.
[33] L. P. Gorkov and E. I. Rashba, Phys. Rev. Lett. **87**, 037004 (2001).
[34] M. Abramowitz and I. A. Stegun, *Handbook of mathematical functions*, (Dover, New York, 1964).